

# AtlasVid : Efficient Ultra-High-Resolution Long Video Generation via Decoupled Global-Local Modeling

Ziyang Mai\*  
 Dartmouth College  
 ziyang.mai.gr@dartmouth.edu

Yuyao Zhang\*  
 Dartmouth College  
 yuyao.zhang.gr@dartmouth.edu

Yu-Wing Tai  
 Dartmouth College

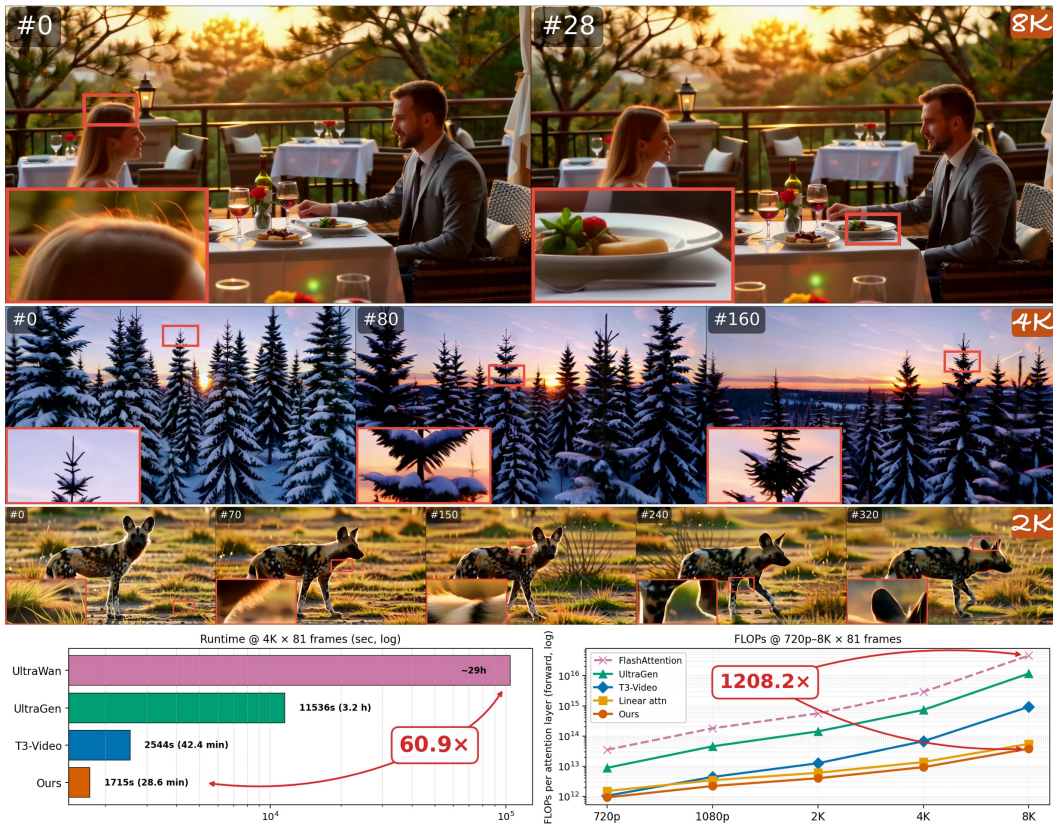


Figure 1: **AtlasVid** enables the generation of ultra-high-resolution and long-duration videos in different settings, including 8K 29 frames, 4K 161 frames and 2K 321 frames. Frame index indicated in the top-left corner and the output resolution in the top-right corner. **Bottom:** AtlasVid runs 60.9× faster than UltraWan at 4K × 81 frames (left) and reduces per-layer attention FLOPs by up to 1208.2× over FlashAttention from 720p to 8K (right).

## Abstract

\*Co-first authors, equal contribution.

Recent diffusion-based video generators have achieved remarkable visual fidelity and prompt controllability, yet scaling them to ultra-high-resolution (UHR) long videos remains prohibitively expensive. The difficulty is especially pronounced for long single-shot generation where a continuous scene must preserve global temporal coherence, and fine-grained spatial details without relying on clip transitions or autoregressive shot stitching. In this work, we revisit this challenge from the perspective of decoupled modeling. We argue that existing video diffusion models already encode strong local visual priors, while the main bottleneck lies in efficiently extending global spatiotemporal modeling as resolution and duration increase. Based on this insight, we propose **AtlasVid**, a decoupled global-local framework for efficient UHR long video generation. **AtlasVid** first generates a low-resolution and low-FPS global semantic proxy via temporally scaled RoPE, thereby extending the temporal horizon without increasing the training token count. Guided by this proxy, a high-resolution detail branch performs joint denoising with hierarchical locality-preserving attention. Reordered spatiotemporal windows preserve geometric locality and asymmetric global-local attention injects aligned semantic guidance and preserves the model’s pretrained ability. This design enables resolution-agnostic training: the model is trained only at 720P with lightweight LoRA adaptation, yet generalizes directly to 4K and beyond for longer (>10s) video synthesis. Experiments show that **AtlasVid** substantially improves the efficiency of ultra-high-resolution long video generation, achieving high-quality UHR long video generation with  $60.9\times$  speed up and significantly less training cost and even better performance than native 4K video generators.

## 1 Introduction

The field of video generation has advanced rapidly, driven by Diffusion Models [Ho et al., 2020] and the Diffusion Transformer (DiT) architecture [Peebles and Xie, 2023]. Recent text-to-video (T2V) systems [Arkhipkin et al., 2025, Chen et al., 2025a, Li et al., 2026, Kong et al., 2024, Team, 2025, Lin et al., 2024, HaCohen et al., 2024, 2026, Ma et al., 2025a, Wan et al., 2025] have significantly improved realism and visual fidelity, enabling compelling video synthesis from text or image prompts. As these models mature, the focus is shifting from prompt following and visual quality toward high-resolution, long-duration generation, motivated by applications in filmmaking, television, and professional content creation, where fine-grained spatial detail and long-range temporal coherence are both critical. To meet this demand, industrial systems [OpenAI, 2025, DeepMind, 2025, Research, 2026, Team, 2026] rely on massive data and computation to support generation up to 2K resolution, typically in a clip-by-clip autoregressive manner. However, each clip is usually limited to less than 5 seconds.

Meanwhile, academic works have explored long-video streaming generation [Yin et al., 2024b, Huang et al., 2025, Chen et al., 2026, Teng et al., 2025] and planning-based methods for extended video creation [Huang et al., 2024a, Zheng et al., 2024, Zhao et al., 2024, Guo et al., 2025], yet genuinely long single-shot generation remains out of reach.

In real-world scenarios, however, high-resolution long single-shot videos are often required, such as cinematic long takes, music and dance performances, and documentary-style footage.

A major challenge is the inherent complexity of the DiT architecture, whose full-attention mechanism scales quadratically with the spatiotemporal input size, i.e.,  $O((HWT)^2)$ , where  $H$ ,  $W$ , and  $T$  denote the height, width, and temporal length of the video. Consequently, doubling all three dimensions increases the computational cost by  $64\times$ .

Moreover, directly training models at ultra-high resolution can introduce additional and unpredictable difficulties such as severe memory pressure, training instability at extremely long token sequences, and the scarcity of native 4K long-video training data. Existing methods [He et al., 2024, Xie et al., 2025, Zhuang et al., 2025] alleviate this issue with a "generation-then-super-resolution" pipeline. However, this "pseudo high-resolution" paradigm mainly improves sharpness and often fails to recover sufficiently rich high-frequency details. Another line of work [Chen et al., 2025b, Zhang et al., 2025c, Wang et al., 2025] improves efficiency through sparse or linearized attention mechanisms, although

Table 1: Training resource comparison with state-of-the-art high-resolution video generation methods.

Method	GPUs	Training Stage	Max Frames	Max Reso.	Duration
UltraWan-4K [Xue et al., 2025]	7.6K H20-hours	LoRA on Wan-1.3B	29f	4K	~1.2s
UltraGen [Hu et al., 2026]	32×H20	4K direct fine-tuning	29f	4K	~1.2s
T3-Video [Zhang et al., 2025a]	64	720P → 4K (two-stage)	81f	4K	~3.4s
<b>AtlasVid (Ours)</b>	<b>2×RTX Pro 6000</b>	<b>720P (+ optional 4K)</b>	<b>321f</b>	<b>&gt;4K</b>	<b>~13.4s</b>

faster, they do not fundamentally resolve the substantial data bottleneck of high-resolution long-video generation.

These limitations prompt a rethinking of what fundamentally restricts high-resolution long-video generation. We hypothesize that pretrained video generation models already possess much of the visual knowledge required to synthesize plausible fine-grained details at higher resolutions, since pretraining exposes them to similar objects, structures, and scenes across different visual scales. From this perspective, the main bottleneck is not an inherent lack of high-resolution generation capacity, but the difficulty of modeling long-range dependencies efficiently as the spatiotemporal resolution grows.

Motivated by this view, we propose a hierarchical locality-preserving attention mechanism for efficient high-resolution long-video generation. Our design decouples the modeling of local neighborhood structure from global semantics, allowing the model to scale more effectively across resolutions. Furthermore, we introduce a temporal-scale RoPE strategy for long-video modeling, which enlarges the temporal modeling range without increasing the token count. By combining hierarchical locality-preserving attention with temporal-scale positional modeling, our framework enables efficient ultra-high-resolution video generation and reduces the data and resource demands of scaling.

- Through the decoupled modeling of global semantic and local details, we significantly reduce the computing complexity of ultra-high-resolution generation leading to a speedup of 60.9× compare to Wan2.1-1.3B baseline.
- Enabled by our resolution-agnostic training paradigm, **AtlasVid** is the first method to jointly scale up both spatial resolution and temporal duration (i.e 4K, 321frames) without the data bottleneck to our knowledge.
- The full pipeline can be trained via LoRA fine-tuning at 720P resolution on as few as **2 NVIDIA RTX Pro 6000 GPUs** and inference on 1 GPU within 29 minutes, with the learned capability transferring directly to 4K inference without any additional high-resolution training stage. In comparison to other method which requires massive training on more than 32 GPUs clusters, **AtlasVid** substantially lowers the resource barrier ultra-high-resolution long video generation.

## 2 Related Work

### 2.1 High Resolution Video Generation

Recent diffusion transformer based video generation models [Wan et al., 2025, Team, 2025, Hong et al., 2022] have demonstrated impressive synthesis quality, yet they are still largely trained at resolutions up to 720P. Scaling these models to ultra-high resolution (UHD), such as 4K, remains challenging due to the quadratic complexity of full attention with respect to token count and the scarcity of high-quality 4K video data. Training-free methods [He et al., 2023, Zhang et al., 2024c, Qiu et al., 2025, Wu et al., 2025] adapt pretrained models to higher resolutions by modifying attention patterns, receptive fields, or positional encodings at inference time. While computationally convenient, they rely entirely on low-resolution priors and often suffer from semantic repetition, over-smoothed textures, and content inconsistency at 4K. Video super-resolution methods [He et al., 2024, Xie et al., 2025, Zhuang et al., 2025] instead cascade low-resolution generation with a dedicated spatial upscaler, but such pipelines are mainly restricted to low-level texture enhancement and cannot reliably correct semantic errors or synthesize genuinely new high-frequency content. Native high-resolution fine-tuning approaches [Xue et al., 2025, Hu et al., 2026, Zhang et al., 2025a, Zhao et al., 2026] directly adapt foundation models on curated high-resolution datasets. However, these methods primarily scale spatial resolution and remain limited to short clips. In contrast, our proposed **AtlasVid** is

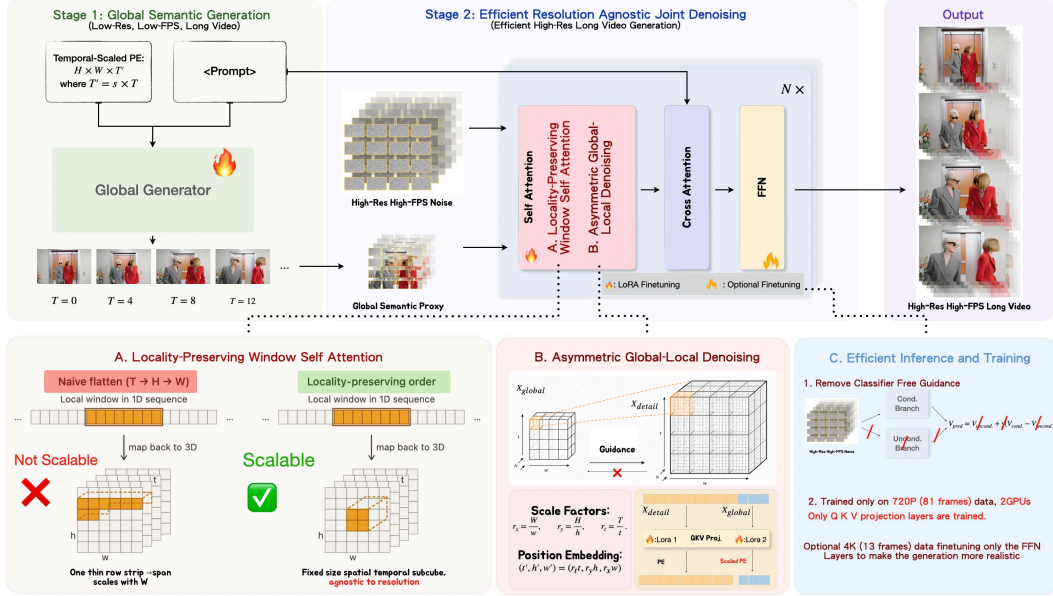


Figure 2: Pipeline of **AtlasVid**. It first employs a semantic generator to produce a low-resolution, low-frame-rate video that serves as a global semantic proxy. Conditioned on this reference, the second stage performs spatiotemporal detail generation through an efficient hierarchical locality-preserving attention mechanism, enabling ultra-high-resolution long-video synthesis (UHRL video) with substantially improved computational efficiency. Section A, B, and C demonstrate the detailed designs for scalable UHRL video generation.

resolution-agnostic: it scales effectively to higher resolutions without relying heavily on native 4K training data.

**Discussion with similar works.** *i) Methodology.* UltraWan, UltraGen, and T3-Video all rely on large-scale 4K data for training. UltraGen adopts carefully designed hierarchical attention modules to reduce computation, while T3-Video uses transformed window attention for more efficient training and inference. In contrast, our method decouples global-local modeling and introduces locality-preserving attention, enabling efficient 4K inference while requiring training only at 720P with optional 4K finetuning for more realistic results. *ii) Training resources.* As shown in Table 1, UltraGen uses 32 H20 GPUs, and T3-Video requires 64 GPUs for training, whereas our method requires only 2 GPUs. *iii) Results.* Our method is the first to enable long single-shot 4K video generation.

## 2.2 Efficient Video Generation

Efficient video generation has attracted increasing attention due to the heavy computational cost of diffusion-based video models, which becomes more prohibitive at ultra high spatial temporal resolutions. Existing methods mainly improve efficiency through several complementary directions. First, hardware-aware attention kernels such as FlashAttention [Dao, 2023, Shah et al., 2024] and SageAttention [Zhang et al., 2024b,a, 2025b] accelerate standard attention computation and reduce memory overhead without changing the model architecture. Second, caching-based methods exploit redundancy across denoising timesteps by reusing intermediate features or attention outputs, thereby reducing repeated computation during sampling [Liu et al., 2024, Ma et al., 2025b, Fan et al., 2025]. Third, many recent approaches improve efficiency at the architectural level by introducing complexity-reduced spatiotemporal modeling, such as training-free sparsification, trainable sparse attention, and linear-complexity designs [Zhang et al., 2025c, Wang et al., 2025, Zhang et al., 2025d]. In addition, distillation-based methods reduce the number of sampling steps for faster deployment [Luo et al., 2023, Yin et al., 2024a]. Different from these works that primarily target general video generation efficiency, our work focuses on native high-resolution video generation and develops sparse-attention-based optimization tailored to low reference guidance setting.

### 3 Method

To generate high-resolution long single-shot videos without incurring the prohibitive quadratic cost of standard self-attention or the substantial training burden of direct high-resolution long-video modeling, **AtlasVid** reformulates spatiotemporal video generation as an efficient hierarchical two-stage pipeline. As illustrated in Figure 2, the first stage employs a semantic generator to produce a low-resolution, low-frame-rate video that serves as a global semantic proxy. Conditioned on this reference, the second stage performs spatiotemporal detail generation through an efficient hierarchical locality-preserving attention mechanism, enabling high-resolution long-video synthesis with substantially improved computational efficiency. In the remainder of this section, Section 3.1 introduces the preliminaries of DiT-based video diffusion models, Section 3.2 presents our decoupled formulation of global semantic and local detail modeling for scalable and efficient generation, and Section 3.3 describes how the global semantic proxy guides high-resolution long-video denoising.

#### 3.1 Preliminaries of DiT based Video Diffusion Models

Most recent DiT-based video generation models adopt a full-attention Transformer architecture to model spatiotemporal dependencies in latent video representations. Given an input video, a 3D-VAE first encodes it into a latent tensor of shape  $D \times T \times H \times W$ , where  $D$  is the channel dimension and  $T, H, W$  denote the temporal and spatial dimensions. The latent tensor is then patchified and flattened into a 1D token sequence of length  $N = THW$ . Full self-attention is applied over the entire sequence, producing an  $N \times N$  attention map with complexity  $O(N^2D)$ . As a result, the cost grows quadratically with the spatiotemporal token count, which quickly becomes prohibitive for high-resolution and long video generation.

#### 3.2 Decoupled Modeling of Global Semantics and Local Details

Generating high-resolution long videos requires simultaneously modeling long-range spatiotemporal dependencies over extremely long token sequences while preserving fine-grained local fidelity. We observe that recent state-of-the-art video generation models already demonstrate strong visual synthesis ability across diverse objects, scales, and motion patterns, suggesting that pretrained models have largely internalized the local visual priors required for detail generation. The main challenge, instead, lies in efficiently maintaining coherent global semantics as the spatiotemporal extent grows. Based on this observation, we decouple global semantic modeling from local detail generation and address them separately in our framework.

**Global Semantic Generation via Temporally Scaled Positions.** The pretrained base model already possesses the capacity to generate low-resolution semantic proxies, but extending such semantic modeling to longer temporal horizons still requires adaptation. A straightforward solution is to finetune the base model for longer video generation directly. However, this quickly becomes prohibitively expensive due to the quadratic complexity of self-attention with respect to temporal token length.

Importantly, global semantic modeling does not require the full frame rate of the target video. Instead, a low-frame-rate video is sufficient to capture the coarse scene evolution and long-range temporal semantics. Based on this observation, we construct the first stage as a low-frame-rate semantic generator. Specifically, we enlarge the temporal indices used in RoPE by a factor of  $r_t$ , such that adjacent generated frames are interpreted as being separated by larger temporal intervals. This allows the model to represent a longer temporal horizon using the same number of frames. For example, when  $r_t = 4$ , a 4fps 20-second semantic proxy has the same temporal token length as an original 5-second video, reducing the self-attention cost by  $16\times$  compared with directly modeling the same duration at the original frame rate. We implement this adaptation by finetuning the base model with LoRA, enabling efficient learning of long-horizon semantic generation while preserving the pretrained visual prior.

**Locality-Preserving Efficient Attention for Detail Generation.** Let the target video contain  $N$  latent tokens. Applying full self-attention over all tokens leads to a quadratic complexity of  $O(N^2)$ , which is prohibitive for high-resolution long-video generation. Existing efficient attention schemes typically reduce this cost by restricting attention to local windows, yielding a complexity of  $O(Nb)$  with window size  $b$ . However, when windows are formed directly on the flattened token sequence,

sequence locality does not necessarily coincide with geometric locality in the original spatiotemporal video volume. As a result, tokens grouped within the same attention window may not belong to the same coherent local region in space and time.

We therefore introduce a locality-preserving efficient attention mechanism for detail generation. Figure 2 (A) demonstrates the differences between ours and naive local-attention. Specifically, given a latent video volume of size  $T \times H \times W$ , we partition it into spatiotemporal cubes of size  $t \times h \times w$ , chosen such that each cube remains within the local generation regime that the pretrained base model can effectively handle. We then reorder the flattened token sequence so that tokens from the same cube become contiguous. Window attention is applied on the reordered sequence with window size  $b = thw$ , ensuring that each sparse attention block corresponds to an actual local spatiotemporal neighborhood.

This construction preserves the computational efficiency of local attention while making the sparse attention pattern compatible with the geometric structure of the video. Consequently, it better preserves the pretrained model’s ability to synthesize fine local details. In practice, we additionally allow attention across adjacent cubes to reduce blocking artifacts near cube boundaries.

### 3.3 Efficient Resolution Agnostic Joint Denoising

Given the global semantic proxy  $X_{\text{global}}$  with length  $n$  and the target noisy video tokens  $X_{\text{detail}}$  with length  $N$ , our next goal is to construct an efficient joint denoising architecture that allows  $X_{\text{global}}$  to guide the generation of  $X_{\text{detail}}$  while remaining scalable across resolutions.

**Efficient Joint Denoising with Hierarchical Attention.** To inject global semantic guidance into high-resolution detail generation, we concatenate the two token streams as  $X = [X_{\text{detail}}; X_{\text{global}}]$ , and perform joint self-attention followed by text cross-attention. The key design principle is an asymmetric hierarchical attention pattern in which the coarse global proxy provides semantic guidance, while the high-resolution detail branch performs denoising under both local detail interactions and global semantic conditioning.

In self-attention,  $X_{\text{global}}$  attends only to itself, while  $X_{\text{detail}}$  attends both to its own tokens through the locality-preserving attention described in Section 3.2 and to the aligned global semantic tokens. The self-attention is formulated as

$$\text{SelfAttn}(Q, K, V) = \text{Softmax}\left(\frac{QK^\top + M}{\sqrt{d}}\right)V, M = \begin{bmatrix} M_{dd} & M_{dg} \\ -\infty & M_{gg} \end{bmatrix} \in \mathbb{R}^{(N+n) \times (N+n)}$$

Here,  $M_{dd}$  denotes the locality-preserving mask for detail-to-detail attention,  $M_{dg}$  denotes the mask for detail-to-global attention, and  $M_{gg}$  denotes unrestricted self-attention among global tokens. The  $-\infty$  block prevents global tokens from attending to detail tokens, thereby enforcing one-way semantic guidance from the global proxy to the noisy detail branch. For text cross-attention, we only allow  $X_{\text{detail}}$  to attend to text tokens. This asymmetric design ensures that the global semantic proxy remains clean and is not corrupted by noisy detail features during denoising.

To adapt the pretrained DiT backbone to this new joint denoising pattern, we apply LoRA finetuning to all the DiT layers associated with global semantic conditioning and to only the query, key, and value projection layers in the detail branch. In contrast, we keep the feed-forward layers in the detail branch frozen in this joint denoising pattern learning process, so that the pretrained model’s original local generative capability is preserved as much as possible while learning the detail-to-global mapping. As an optional refinement stage, we additionally finetune previously frozen FFN layers using a small and short (13-frame) videos to further improve local realism.

**Scaled Spatial-Temporal RoPE for Global-Local Matching.** To make the global semantic proxy provide accurate guidance for high-resolution detail generation, we align its positional encoding with the coordinate system of the target video. Demonstrated in Figure 2 (B), for a global proxy token located at spatial-temporal index  $(w', h', t')$ , we scale its RoPE coordinates by

$$r_x = \frac{W}{w'}, \quad r_y = \frac{H}{h'}, \quad r_t = \frac{T}{t'}$$

so that its position is mapped to the corresponding location in the high-resolution long-video latent grid. In this way, each token in  $X_{\text{global}}$  serves as an anchor for the corresponding spatiotemporal cube in  $X_{\text{detail}}$ , enabling consistent global-to-local semantic guidance during denoising.



Figure 3: Qualitative comparison of long ultra-high-resolution video generation. Top: The first two rows compare **AtlasVid** with SkyReels-V2 at 720P and T3-Video at 4K. All three methods generate 161-frame results. T3-Video exhibits structural artifacts, color shifts, and quality degradation when extended to 161 frames, whereas **AtlasVid** maintains coherent structures and stable visual quality. Bottom: Rows 3–5 show the 81-frame comparison with UltraGen at 1080P and T3-Video at 4K. **AtlasVid** preserves 4K-level details and is the only method that scales reliably beyond 81 frames.

This positional alignment naturally complements the asymmetric hierarchical attention described above: the global proxy provides semantically aligned coarse guidance, while the detail branch focuses on synthesizing local high-frequency content within each spatiotemporal neighborhood. Since our framework explicitly decouples global semantic modeling from local detail generation, training only needs to learn the new locality-preserving attention pattern and the hierarchical global-local correspondence, rather than directly modeling the full target spatiotemporal scale end-to-end.

As a result, **AtlasVid** does not require long ultra-high-resolution videos (e.g., 4K, 321-frame videos) for training as illustrated in Figure 2(c), making the overall training pipeline resolution-agnostic and scalable. Moreover, due to the existence of the global proxy as condition, we remove the Classifier-Free Guidance which significantly speeds up the inference.

## 4 Experiments

### 4.1 Implementation Details

**Training details.** We implement **AtlasVid** on top of Wan2.1-1.3B for both stage 1 and stage 2. Models are trained on UltraVideo using AdamW optimizer for 15K iterations (Batch size 1) on 2 RTX 6000 Ada GPUs with gradient accumulation 4. Learning rates is  $1e-4$  with LoRA rank 16. Models are trained on 720p, 81 frames, and is successfully scaled beyond 4K, 321frames. Stage 1 fine-tunes the base model with temporal-scale RoPE ( $r_t=4$ ) for long-horizon low frame-rate semantic generation. We set the spatial-temporal block size in stage 2 to be (256, 256, 32) which is equivalent to (8, 8, 4) in the latent space and adapts a smaller block-size for the border cases when the spatial-temporal

resolution cannot be divided by the block-size. We adapt the mask rule for flex attention to support dynamic length and resolution.

**Baselines.** We compare against: Wan2.1-T2V-1.3B [Wan et al., 2025], UltraWan [Xue et al., 2025], UltraGen [Hu et al., 2026], and T3-Video-T2V-1.3B [Zhang et al., 2025a]. Note that neither Wan2.1-T2V-1.3B, nor UltraGen have released official 4K-resolution checkpoints, we therefore evaluate them at their highest support resolution, 720p and 1080p separately.

## 4.2 Qualitative Results

**Demonstration of UHR long videos.** Figure 1 presents examples of ultra-high-resolution long videos generated by our method, reaching up to 8K resolution and 321 frames in temporal length. These results demonstrate the scalability of our framework in both spatial resolution and temporal duration, while maintaining coherent scene structure and fine-grained visual details.

**Comparison on 4K long videos** Figure 3 provides qualitative comparisons for long 4K video generation. The upper section compares long video generation ability on 161 frames with the long-video generator SkyReels-V2 under 720p and the native 4K generator T3-Video under 4K. Our method is the only one that produces plausible long 4K results. When extrapolated to longer temporal lengths, T3-Video exhibits noticeable quality degradation and prompt misalignment, such as color shift and incorrectly changing the prompted man into a woman. SkyReels-V2 can generate long video with consistency, but their result are limited to 720p. The lower section further compares our method with native UHR video generation methods, including UltraGen and T3-Video. UltraGen produces noticeably inconsistent results when using its released 1080P checkpoint, such as the feather on the head in green box. Though our method and T3-Video preserve detailed structures at 4K resolution, T3-Video still exhibits structural artifacts, such as distorted bird shape in green and yellow box, with extra legs in blue box, due to the lack of explicit global semantic control. In contrast, our decoupled design provides stable semantic guidance and more coherent high-resolution long-video synthesis.

## 4.3 Quantitative Results

Table 2 reports quantitative results using both VBench and high-resolution evaluation metrics, with detailed metric definitions provided in the appendix. We randomly sample 100 prompts from VBench as our test set. Wan2.1 and UltraGen are evaluated at 720P and 1080P respectively, as their 4K checkpoints are not publicly available, while UltraWan, T3-Video, and **AtlasVid** are evaluated at 4K resolution. **AtlasVid** achieves the best performance on most VBench metrics among existing 4K generation methods, and remains competitive with pretrained models evaluated at 720P resolution. These results demonstrate the strong capability of **AtlasVid** in synthesizing high-quality ultra-high-resolution videos while preserving both visual fidelity and temporal consistency.

Table 2: Quantitative comparison on 4K long video generation. Our method achieves the best performance among 4K generation methods and remains competitive with 720P base models.

Method	4K HD Metrics			VBench Motion					VBench Semantics		
	HD-FVD↓	HD-LPIPS↑	CLIP↑	SC↑	BC↑	TF↑	MS↑	DD↑	AQ↑	IQ↑	Clr.↑
Wan2.1	512.32	0.6424	0.3076	96.34	97.29	99.49	97.44	<b>85.56</b>	62.43	66.51	89.58
UltraGen	432.71	0.6358	0.2848	94.19	96.33	98.90	98.72	71.34	58.13	65.88	97.13
UltraWan	372.39	0.6211	0.2903	95.71	<b>97.94</b>	98.86	99.06	62.22	59.52	67.39	<b>99.10</b>
T3-Video	311.29	0.6471	0.2972	97.02	96.23	95.12	99.17	78.92	62.96	68.17	97.42
<b>Ours</b>	<b>284.71</b>	<b>0.6695</b>	<b>0.3019</b>	<b>97.41</b>	96.54	<b>99.57</b>	<b>99.31</b>	82.21	<b>63.31</b>	<b>68.52</b>	98.31

**Efficiency Comparisons.** We also compare our model’s efficiency against the other baselines. The bottom part of Figure 1 demonstrates the comparison among our attention and other attention mechanisms across 720P to 8K resolutions (81 frames), where our attention even beats linear attention in terms of floating point operations (FLOPs) and surpasses dense attention by 1208.2 times. The right part demonstrates the overall inference time comparison on 4K 81 frames, given the efficient designs we achieve 1.48× faster than T3-Video and 60.9× faster than baseline.



Figure 4: Ablation on the importance of our attention design. The first two columns demonstrate the effect of global guidance. The third and fourth columns evaluate our locality-preserving attention, where attention to neighboring spatiotemporal blocks is removed to better visualize the learned block structure. All models are trained at 720P and evaluated at 4K.

## 5 Ablation Study

**Ablation on different attention patterns.** We conduct ablation studies on different attention patterns to validate our design choices, with all variants trained only on 720P data. The left part shows that removing the global proxy guidance leads to inconsistent generation results, highlighting the importance of global semantic conditioning. The right part demonstrates the role of locality-preserving attention in extrapolating beyond the training resolution. For clearer visualization, we remove attention to neighboring blocks in this ablation so the "blocks" will be shown in the figure. With our locality-preserving attention, the model successfully scales to 4K generation, whereas naive block attention fails to generalize. These results confirm the effectiveness of our global-local design and locality-preserving attention mechanism.

**Ablation on 4K data fine-tuning.** Figure 5 compares videos generated by models trained with and without additional 4K real data. Even without 4K fine-tuning, our model already produces clear 4K textures, demonstrating the resolution extrapolation ability of our framework. Additional 4K fine-tuning further improves naturalness and local realism, and is therefore used only as an optional refinement stage. Importantly, this stage is substantially lighter than the native 4K training required by UltraGen and T3-Video: instead of using long 4K 81-frame videos, we only require short 4K 13-frame clips to adapt the feed-forward layers toward more natural high-resolution pixel synthesis.

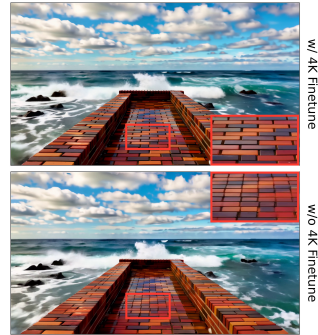


Figure 5: Ablation study on 4K data finetuning. With 4K finetuning (top), the model produces more realistic fine-grained details, while without 4K finetuning (bottom) it can still generate plausible details, demonstrating the robustness of our base model.

**Limitations.** Our framework relies on the Stage-1 semantic generator to produce the global proxy, and thus errors or artifacts introduced at this stage may be inherited by the final high-resolution output. In addition, although our decoupled design substantially improves scalability, the final quality still depends on the alignment between the low-resolution proxy and the high-resolution detail branch. In the future we may try larger scale training on more resources and larger dataset to obtain even better results. Our method is also orthogonal to other acceleration techniques like distillation, which may further speed up our method.

## 6 Conclusion

We presented **AtlasVid**, an efficient framework for ultra-high-resolution long video generation. By decoupling global semantic modeling from local detail synthesis, **AtlasVid** avoids directly applying full attention to prohibitively large spatiotemporal token sequences. A low-resolution, low-frame-rate semantic proxy captures long-range scene evolution, while a high-resolution detail branch performs coordinate-aligned joint denoising with hierarchical locality-preserving attention. This design enables resolution-agnostic training: with lightweight LoRA adaptation mainly at 720P, **AtlasVid** generalizes to 4K and beyond while substantially reducing computation. Experiments demonstrate that **AtlasVid** produces coherent, detailed ultra-high-resolution long videos with significantly improved efficiency, offering a scalable path toward accessible ultra-high-resolution video generation.

## References

- Vladimir Arkhipkin, Vladimir Korviakov, Nikolai Gerasimenko, Denis Parkhomenko, Viacheslav Vasilev, Alexey Letunovskiy, Nikolai Vaulin, Maria Kovaleva, Ivan Kirillov, Lev Novitskiy, et al. Kandinsky 5.0: A family of foundation models for image and video generation. *arXiv preprint arXiv:2511.14993*, 2025.
- Mathilde Caron, Hugo Touvron, Ishan Misra, Hervé Jégou, Julien Mairal, Piotr Bojanowski, and Armand Joulin. Emerging properties in self-supervised vision transformers. In *Proceedings of the IEEE/CVF international conference on computer vision*, pages 9650–9660, 2021.
- Joao Carreira and Andrew Zisserman. Quo vadis, action recognition? a new model and the kinetics dataset. In *proceedings of the IEEE Conference on Computer Vision and Pattern Recognition*, pages 6299–6308, 2017.
- Guibin Chen, Dixuan Lin, Jiangping Yang, Chunze Lin, Junchen Zhu, Mingyuan Fan, Hao Zhang, Sheng Chen, Zheng Chen, Chengcheng Ma, et al. Skyreels-v2: Infinite-length film generative model. *arXiv preprint arXiv:2504.13074*, 2025a.
- Junsong Chen, Yuyang Zhao, Jincheng Yu, Ruihang Chu, Junyu Chen, Shuai Yang, Xianbang Wang, Yicheng Pan, Daquan Zhou, Huan Ling, et al. Sana-video: Efficient video generation with block linear diffusion transformer. *arXiv preprint arXiv:2509.24695*, 2025b.
- Shuo Chen, Cong Wei, Sun Sun, Ping Nie, Kai Zhou, Ge Zhang, Ming-Hsuan Yang, and Wenhui Chen. Context forcing: Consistent autoregressive video generation with long context. *arXiv preprint arXiv:2602.06028*, 2026.
- Tri Dao. Flashattention-2: Faster attention with better parallelism and work partitioning. *arXiv preprint arXiv:2307.08691*, 2023.
- Google DeepMind. Veo 3.1: Advancing cinematic video generation with native audio and 4k resolution. Technical report, Google DeepMind, October 2025. URL <https://deepmind.google/technologies/veo/>.
- Zhentao Fan, Zongzuo Wang, and Weiwei Zhang. Taocache: Structure-maintained video generation acceleration. *arXiv preprint arXiv:2508.08978*, 2025.
- Yuwei Guo, Ceyuan Yang, Ziyan Yang, Zhibei Ma, Zhijie Lin, Zhenheng Yang, Dahua Lin, and Lu Jiang. Long context tuning for video generation. In *Proceedings of the IEEE/CVF International Conference on Computer Vision*, pages 17281–17291, 2025.
- Yoav HaCohen, Nisan Chiprut, Benny Brazowski, Daniel Shalem, Dudu Moshe, Eitan Richardson, Eran Levin, Guy Shiran, Nir Zabari, Ori Gordon, Poriya Panet, Sapir Weissbuch, Victor Kulikov, Yaki Bitterman, Zeev Melumian, and Ofir Bibi. Ltx-video: Realtime video latent diffusion. *arXiv preprint arXiv:2501.00103*, 2024.
- Yoav HaCohen, Benny Brazowski, Nisan Chiprut, Yaki Bitterman, Andrew Kvochko, Avishai Berkowitz, Daniel Shalem, Daphna Lifschitz, Dudu Moshe, Eitan Porat, et al. Ltx-2: Efficient joint audio-visual foundation model. *arXiv preprint arXiv:2601.03233*, 2026.
- Jingwen He, Tianfan Xue, Dongyang Liu, Xinqi Lin, Peng Gao, Dahua Lin, Yu Qiao, Wanli Ouyang, and Ziwei Liu. Venhancer: Generative space-time enhancement for video generation. *arXiv preprint arXiv:2407.07667*, 2024.
- Yingqing He, Shaoshu Yang, Haoxin Chen, Xiaodong Cun, Menghan Xia, Yong Zhang, Xintao Wang, Ran He, Qifeng Chen, and Ying Shan. Scalecrafter: Tuning-free higher-resolution visual generation with diffusion models. In *The Twelfth International Conference on Learning Representations*, 2023.
- Jonathan Ho, Ajay Jain, and Pieter Abbeel. Denoising diffusion probabilistic models. *Advances in neural information processing systems*, 33:6840–6851, 2020.
- Wenyi Hong, Ming Ding, Wendi Zheng, Xinghan Liu, and Jie Tang. Cogvideo: Large-scale pretraining for text-to-video generation via transformers. *arXiv preprint arXiv:2205.15868*, 2022.

- Teng Hu, Jiangning Zhang, Zihan Su, and Ran Yi. Ultragen: High-resolution video generation with hierarchical attention. In *Proceedings of the AAAI Conference on Artificial Intelligence*, volume 40, pages 4923–4931, 2026.
- Lianghua Huang, Wei Wang, Zhi-Fan Wu, Yupeng Shi, Huanzhang Dou, Chen Liang, Yutong Feng, Yu Liu, and Jingren Zhou. In-context lora for diffusion transformers. *arXiv preprint arXiv:2410.23775*, 2024a.
- Xun Huang, Zhengqi Li, Guande He, Mingyuan Zhou, and Eli Shechtman. Self forcing: Bridging the train-test gap in autoregressive video diffusion. *arXiv preprint arXiv:2506.08009*, 2025.
- Ziqi Huang, Yanan He, Jiashuo Yu, Fan Zhang, Chenyang Si, Yuming Jiang, Yuanhan Zhang, Tianxing Wu, Qingyang Jin, Nattapol Chanpaisit, Yaohui Wang, Xinyuan Chen, Limin Wang, Dahua Lin, Yu Qiao, and Ziwei Liu. VBench: Comprehensive benchmark suite for video generative models. In *Proceedings of the IEEE/CVF Conference on Computer Vision and Pattern Recognition*, 2024b.
- Junjie Ke, Qifei Wang, Yilin Wang, Peyman Milanfar, and Feng Yang. Musiq: Multi-scale image quality transformer. In *Proceedings of the IEEE/CVF international conference on computer vision*, pages 5148–5157, 2021.
- Weijie Kong, Qi Tian, Zijian Zhang, Rox Min, Zuozhuo Dai, Jin Zhou, Jiangfeng Xiong, Xin Li, Bo Wu, Jianwei Zhang, et al. Hunyuanvideo: A systematic framework for large video generative models. *arXiv preprint arXiv:2412.03603*, 2024.
- Debang Li, Zhengcong Fei, Tuanhui Li, Yikun Dou, Zheng Chen, Jiangping Yang, Mingyuan Fan, Jingtao Xu, Jiahua Wang, Baoxuan Gu, et al. Skyreels-v3 technique report. *arXiv preprint arXiv:2601.17323*, 2026.
- Zhen Li, Zuo-Liang Zhu, Ling-Hao Han, Qibin Hou, Chun-Le Guo, and Ming-Ming Cheng. Amt: All-pairs multi-field transforms for efficient frame interpolation. In *Proceedings of the IEEE/CVF Conference on Computer Vision and Pattern Recognition*, pages 9801–9810, 2023.
- Bin Lin, Yunyang Ge, Xinhua Cheng, Zongjian Li, Bin Zhu, Shaodong Wang, Xianyi He, Yang Ye, Shenghai Yuan, Liuhan Chen, et al. Open-sora plan: Open-source large video generation model. *arXiv preprint arXiv:2412.00131*, 2024.
- Feng Liu, Shiwei Zhang, Xiaofeng Wang, Yujie Wei, Haonan Qiu, Yuzhong Zhao, Yingya Zhang, Qixiang Ye, and Fang Wan. Timestep embedding tells: It’s time to cache for video diffusion model. *arXiv preprint arXiv:2411.19108*, 2024.
- Simian Luo, Yiqin Tan, Longbo Huang, Jian Li, and Hang Zhao. Latent consistency models: Synthesizing high-resolution images with few-step inference. *arXiv preprint arXiv:2310.04378*, 2023.
- Guoqing Ma, Haoyang Huang, Kun Yan, Liangyu Chen, Nan Duan, Shengming Yin, Changyi Wan, Ranchen Ming, Xiaoni Song, Xing Chen, et al. Step-video-t2v technical report: The practice, challenges, and future of video foundation model. *arXiv preprint arXiv:2502.10248*, 2025a.
- Zehong Ma, Longhui Wei, Feng Wang, Shiliang Zhang, and Qi Tian. Magcache: Fast video generation with magnitude-aware cache. *arXiv preprint arXiv:2506.09045*, 2025b.
- OpenAI. Sora 2 technical report: Expanding capabilities in media generation. Technical report, OpenAI, 2025. URL <https://openai.com/research/video-generation-models-as-world-simulators>.
- William Peebles and Saining Xie. Scalable diffusion models with transformers. In *Proceedings of the IEEE/CVF international conference on computer vision*, pages 4195–4205, 2023.
- Haonan Qiu, Ning Yu, Ziqi Huang, Paul Debevec, and Ziwei Liu. Cinescale: Free lunch in high-resolution cinematic visual generation. *arXiv preprint arXiv:2508.15774*, 2025.
- ByteDance Research. Seedance 2.0: A unified multimodal director for narrative video synthesis. Technical report, ByteDance, February 2026. URL <https://seed.bytedance.com/>.

- Jay Shah, Ganesh Bikshandi, Ying Zhang, Vijay Thakkar, Pradeep Ramani, and Tri Dao. Flashattention-3: Fast and accurate attention with asynchrony and low-precision. *Advances in Neural Information Processing Systems*, 37:68658–68685, 2024.
- Kuaishou Technology AI Team. Kling 3.0: High-fidelity video generation with physics-aware motion and omni-native audio. Technical report, Kuaishou Technology, February 2026. URL <https://klingai.com/>.
- Tencent Hunyuan Foundation Model Team. Hunyuanvideo 1.5 technical report, 2025. URL <https://arxiv.org/abs/2511.18870>.
- Zachary Teed and Jia Deng. Raft: Recurrent all-pairs field transforms for optical flow. In *European conference on computer vision*, pages 402–419. Springer, 2020.
- Hansi Teng, Hongyu Jia, Lei Sun, Lingzhi Li, Maolin Li, Mingqiu Tang, Shuai Han, Tianning Zhang, WQ Zhang, Weifeng Luo, et al. Magi-1: Autoregressive video generation at scale. *arXiv preprint arXiv:2505.13211*, 2025.
- Team Wan, Ang Wang, Baole Ai, Bin Wen, Chaojie Mao, Chen-Wei Xie, Di Chen, Feiwu Yu, Haiming Zhao, Jianxiao Yang, et al. Wan: Open and advanced large-scale video generative models. *arXiv preprint arXiv:2503.20314*, 2025.
- Hongjie Wang, Chih-Yao Ma, Yen-Cheng Liu, Ji Hou, Tao Xu, Jialiang Wang, Felix Juefei-Xu, Yaqiao Luo, Peizhao Zhang, Tingbo Hou, et al. Lingen: Towards high-resolution minute-length text-to-video generation with linear computational complexity. In *Proceedings of the Computer Vision and Pattern Recognition Conference*, pages 2578–2588, 2025.
- Jialian Wu, Jianfeng Wang, Zhengyuan Yang, Zhe Gan, Zicheng Liu, Junsong Yuan, and Lijuan Wang. Grit: A generative region-to-text transformer for object understanding. In *European Conference on Computer Vision*, pages 207–224. Springer, 2024.
- Yunfeng Wu, Jiayi Song, Zhenxiong Tan, Zihao He, and Songhua Liu. Freeswim: Revisiting sliding-window attention mechanisms for training-free ultra-high-resolution video generation. *arXiv preprint arXiv:2511.14712*, 2025.
- Rui Xie, Yinhong Liu, Penghao Zhou, Chen Zhao, Jun Zhou, Kai Zhang, Zhenyu Zhang, Jian Yang, Zhenheng Yang, and Ying Tai. Star: Spatial-temporal augmentation with text-to-video models for real-world video super-resolution. In *Proceedings of the IEEE/CVF International Conference on Computer Vision*, pages 17108–17118, 2025.
- Zhucun Xue, Jiangning Zhang, Teng Hu, Haoyang He, Yinan Chen, Yuxuan Cai, Yabiao Wang, Chengjie Wang, Yong Liu, Xiangtai Li, et al. Ultravideo: High-quality uhd video dataset with comprehensive captions. *arXiv preprint arXiv:2506.13691*, 2025.
- Tianwei Yin, Michaël Gharbi, Richard Zhang, Eli Shechtman, Fredo Durand, William T Freeman, and Taesung Park. One-step diffusion with distribution matching distillation. In *Proceedings of the IEEE/CVF conference on computer vision and pattern recognition*, pages 6613–6623, 2024a.
- Tianwei Yin, Qiang Zhang, Richard Zhang, William T Freeman, Fredo Durand, Eli Shechtman, and Xun Huang. From slow bidirectional to fast causal video generators. *arXiv e-prints*, pages arXiv–2412, 2024b.
- Jiangning Zhang, Junwei Zhu, Teng Hu, Yabiao Wang, Donghao Luo, Weijian Cao, Zhenye Gan, Xiaobin Hu, Zhucun Xue, and Chengjie Wang. Transform trained transformer: Accelerating naive 4k video generation over 10x. *arXiv preprint arXiv:2512.13492*, 2025a.
- Jintao Zhang, Haofeng Huang, Pengl Zhang, Jia Wei, Jun Zhu, and Jianfei Chen. Sageattention2: Efficient attention with thorough outlier smoothing and per-thread int4 quantization. *arXiv preprint arXiv:2411.10958*, 2024a.
- Jintao Zhang, Jia Wei, Haofeng Huang, Pengl Zhang, Jun Zhu, and Jianfei Chen. Sageattention: Accurate 8-bit attention for plug-and-play inference acceleration. *arXiv preprint arXiv:2410.02367*, 2024b.

- Jintao Zhang, Jia Wei, Pengle Zhang, Xiaoming Xu, Haofeng Huang, Haoxu Wang, Kai Jiang, Jianfei Chen, and Jun Zhu. Sageattention3: Microscaling fp4 attention for inference and an exploration of 8-bit training. *arXiv preprint arXiv:2505.11594*, 2025b.
- Jintao Zhang, Chendong Xiang, Haofeng Huang, Jia Wei, Haocheng Xi, Jun Zhu, and Jianfei Chen. Spargeattn: Accurate sparse attention accelerating any model inference. *arXiv e-prints*, pages arXiv-2502, 2025c.
- Peiyuan Zhang, Yongqi Chen, Haofeng Huang, Will Lin, Zhengzhong Liu, Ion Stoica, Eric Xing, and Hao Zhang. Vsa: Faster video diffusion with trainable sparse attention. *arXiv preprint arXiv:2505.13389*, 2025d.
- Shen Zhang, Zhaowei Chen, Zhenyu Zhao, Yuhao Chen, Yao Tang, and Jiajun Liang. Hidiffusion: Unlocking higher-resolution creativity and efficiency in pretrained diffusion models. In *European Conference on Computer Vision*, pages 145–161. Springer, 2024c.
- Canyu Zhao, Mingyu Liu, Wen Wang, Weihua Chen, Fan Wang, Hao Chen, Bo Zhang, and Chunhua Shen. Moviedreamer: Hierarchical generation for coherent long visual sequence. *arXiv preprint arXiv:2407.16655*, 2024.
- Chen Zhao, Jiawei Chen, Hongyu Li, Zhuoliang Kang, Shilin Lu, Xiaoming Wei, Kai Zhang, Jian Yang, and Ying Tai. Luve: Latent-cascaded ultra-high-resolution video generation with dual frequency experts. *arXiv preprint arXiv:2602.11564*, 2026.
- Mingzhe Zheng, Yongqi Xu, Haojian Huang, Xuran Ma, Yexin Liu, Wenjie Shu, Yatian Pang, Feilong Tang, Qifeng Chen, Harry Yang, et al. Videogen-of-thought: A collaborative framework for multi-shot video generation. *arXiv preprint arXiv:2412.02259*, 3(6), 2024.
- Junhao Zhuang, Shi Guo, Xin Cai, Xiaohui Li, Yihao Liu, Chun Yuan, and Tianfan Xue. Flashvsr: Towards real-time diffusion-based streaming video super-resolution. *arXiv preprint arXiv:2510.12747*, 2025.

## A More Results

Here we presents more results on 4K 161 frames, 2K 321 frames and 8K 29 frames in Figure 6, Figure 7, Figure 8, Figure 9 and Figure 10. We will include the videos in the supplementary materials.

## B Extended Implementation Details

### B.1 Training Configuration

We build **AtlasVid** on top of Wan2.1-T2V-1.3B Wan et al. [2025] and train both stages with LoRA rank 16 using the AdamW optimizer (learning rate  $1 \times 10^{-4}$ ,  $\beta_1=0.9$ ,  $\beta_2=0.95$ , weight decay 0.01). All training is conducted on  $2 \times$  NVIDIA RTX Pro 6000 (Ada) GPUs, batch size 1 per GPU with gradient accumulation 4 (effective batch size 8) for 15K iterations. Mixed-precision (bf16) is used throughout, and we adopt a flow-matching objective consistent with the Wan2.1 base model.

**Stage 1 (semantic generator).** We finetune the base model with temporal-scale RoPE ( $r_t=4$ ) on  $720P \times 81$ -frame clips sub-sampled at 4 fps, so that an 81-frame proxy spans an effective horizon of  $\sim 20$  seconds at 16 fps target frame rate.

**Stage 2 (detail branch).** The latent volume is partitioned into spatiotemporal cubes of pixel size (256, 256, 32), equivalent to (8, 8, 4) in the 4D latent grid produced by the Wan2.1 3D-VAE. Border cubes that cannot be evenly tiled adopt a smaller block size automatically. We implement the asymmetric mask  $M$  (§3.3) on top of PyTorch `flex_attention` so that the kernel supports dynamic resolution and length without re-compilation per shape.

**Optional 4K refinement.** The optional FFN refinement stage finetunes only the feed-forward layers of the detail branch on 13-frame  $3840 \times 2160$  clips drawn from UltraVideo Xue et al. [2025], for 2K iterations at the same learning rate.

### B.2 Inference Configuration

Unless stated otherwise, all reported numbers and figures use Euler sampler and *disable* classifier-free guidance (CFG), which is justified by the ablation in (§5 of the main paper. We perform inference on a single RTX Pro 6000. End-to-end runtime includes text encoding, both denoising stages, and 3D-VAE decoding.

## C Detailed Metric Definitions

This section formalises the metrics referenced in Table 2 and the ablation tables of the main paper. For all metrics,  $v \in \mathbb{R}^{T \times H \times W \times 3}$  denotes a video. Higher-is-better metrics are marked  $\uparrow$  and lower-is-better  $\downarrow$ .

### C.1 High-Definition Metrics

The HD-FVD, HD-LPIPS, and HD-MSE metrics are designed for ultra-high-resolution video evaluation, where standard FVD/LPIPS are constrained by the  $224 \times 224$  input size of their backbones. We follow the formulation introduced by UltraGen Hu et al. [2026].

**HD-FVD**  $\downarrow$  Standard FVD computes the Fréchet distance between I3D Carreira and Zisserman [2017] feature distributions of generated and reference videos. Because I3D operates on  $224 \times 224$  inputs, naively resizing a 4K clip to  $224^2$  destroys all high-frequency content. HD-FVD instead splits each frame into a regular grid of non-overlapping  $H_l \times W_l$  patches with  $H_l \approx W_l \approx 224$ , extracts I3D features per spatiotemporal patch tube, and reports

$$\text{HD-FVD} = \text{FD}\left(\mathcal{N}(\mu_g, \Sigma_g) \parallel \mathcal{N}(\mu_r, \Sigma_r)\right),$$

where  $(\mu_g, \Sigma_g)$  and  $(\mu_r, \Sigma_r)$  are the means and covariances of generated and reference patch-feature distributions, and  $\text{FD}(\cdot \parallel \cdot)$  is the Fréchet distance. We use the public Kinetics-pretrained I3D checkpoint and patch each  $T = 16$ -frame clip into  $3 \times 3$  spatial patches at 4K (covering the full frame).



The video opens with a wide shot of a tranquil park setting, focusing on a picturesque pond. At the center...



The video captures a bird with a vividly contrasting black, white, and blue plumage, perched gracefully on a slender branch...



The video captures a lively scene at a playground where four children are engaged in the simple joy of swinging....



The video begins with a wide-angle shot of the ancient ruins of Palmyra, highlighting the grandeur of the remaining columns...



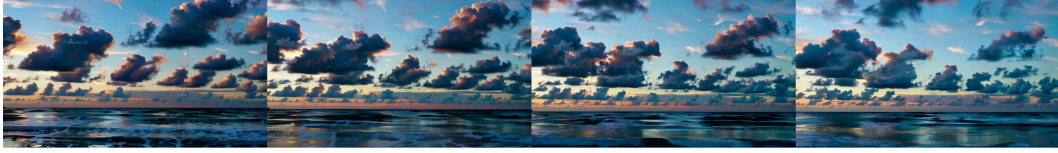
The video captures a dynamic interaction between a woman and a man seated across from each other at a sleek,...



The video captures a serene and aesthetically pleasing interior space characterized by its modern architectural design. The scene begins with...



The video captures a serene scene of a flock of bar-headed geese in a lush, expansive grassy field. The geese,...



The video opens with a wide shot of the ocean, its surface gently rippling under the fading light of the...

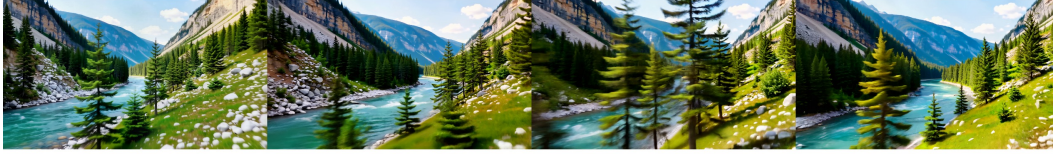


The video showcases a formal concert scene where two women, dressed in glamorous evening gowns, are on stage engaging with...

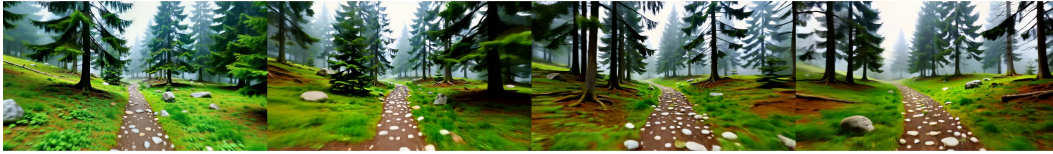
Figure 6: 4K 161 Frames results: Each results spans one row. Examples show no quality degradation or color drift. The frame indices are 0, 53, 106, and 160.



The video opens with a sweeping aerial shot of a majestic mountain peak, capturing its grandeur against the backdrop of...



The video begins with a wide-angle shot that captures the vastness of the mountainous landscape. The camera slowly pans across...



The video begins with a wide shot of a narrow, rocky path cutting through a dense forest. The path is...



The video captures a serene and picturesque scene featuring a young girl dressed in a cowboy hat and denim overalls,...



The video opens with a wide shot of the ocean floor, setting the stage for the tranquil underwater environment. As...



The video opens with a wide shot of a majestic iceberg dominating the frame, its intricate textures and varying shades...



The video opens with a serene view of a dense forest, filled with vibrant green foliage and tall trees that...



The video showcases a man engaged in the process of food preparation in an outdoor setting. He stands at a...



The video captures a man dressed in a sleek black suit as he confidently strides through an opulent interior setting,...

Figure 7: 4K 161 Frames results: Each results spans one row. Examples show no quality degradation or color drift. The frame indices are 0, 53, 106, and 160.



Figure 8: 2K 321 Frames results: Each results spans for two rows. The examples here shows large continuous camera movements. The frame indices are 0, 45, 91, 137, 182, 228, 274 and 320.



Figure 9: 2K 321 Frames results: Each results spans for two rows. The examples here shows large continuous camera movements. The frame indices are 0, 45, 91, 137, 182, 228, 274 and 320.



The video begins with a close-up shot of a pelican,...



The video showcases a fascinating underwater scene featuring a small...

Figure 10: 8K 29 Frames results: Each results spans for two rows. The frame indices are 0 and 28.

Specifically, we apply the same evaluation algorithm to both Wan2.1 (720p) and UltraGen (1080p), which results in relatively high HD-FVD scores. This is because the patch distributions of low-resolution and high-resolution videos differ significantly.

**HD-LPIPS**  $\uparrow$  This *no-reference* metric quantifies how much high-frequency content is preserved in a generated video by measuring its perceptual distance from progressively low-pass-filtered copies of itself. Let  $v_t$  denote the  $t$ -th frame of a video  $V$  of length  $T$ , and let  $v_{t,D,2^k}$  denote  $v_t$  bilinearly down-sampled by a factor of  $2^k$  and then bilinearly up-sampled back to the original resolution. We define

$$\text{HD-LPIPS}(V) = \frac{1}{T} \sum_{t=1}^T \sum_{k \in \mathcal{K}} \text{LPIPS}(v_t, v_{t,D,2^k}),$$

where  $\mathcal{K} = \{3, 4, 5\}$  corresponds to down-sampling factors of 8, 16, and 32, chosen to capture detail across multiple spatial scales while avoiding both noise-dominated (small factors) and structure-dominated (large factors) regimes. A higher HD-LPIPS indicates that the generated video differs more from its low-pass-filtered versions, suggesting richer high-frequency content. We note that this metric reflects high-frequency energy in general, and should therefore be interpreted alongside HD-FVD and perceptual quality metrics to disambiguate genuine fine detail from high-frequency artifacts.

## C.2 Text Video Alignment

**CLIP**  $\uparrow$ . We report frame-averaged cosine similarity between the prompt embedding and per-frame visual embeddings. For a video with  $T$  frames and prompt  $p$ ,

$$\text{CLIP}(v, p) = \frac{1}{T} \sum_{t=1}^T \frac{\langle f_{\text{img}}(v_t), f_{\text{txt}}(p) \rangle}{\|f_{\text{img}}(v_t)\| \|f_{\text{txt}}(p)\|}.$$

## C.3 VBench Dimensions

We follow the VBench Huang et al. [2024b] protocol and report the eight dimensions used in Table 2. All scores lie in  $[0, 1]$  and higher is better.

- **Subject Consistency (SC)** — frame-to-frame DINO Caron et al. [2021] cosine similarity of the foreground subject; measures whether the subject identity is preserved across the clip.
- **Background Consistency (BC)** — frame-to-frame CLIP image cosine similarity of the background region; measures scene stability.
- **Temporal Flickering (TF)** — mean absolute pixel difference between consecutive frames in static regions; rewards low flicker.
- **Motion Smoothness (MS)** — drops every other frame, interpolates it back with the AMT Li et al. [2023] video frame interpolation model, and reports the inverse reconstruction error; rewards physically plausible motion.
- **Dynamic Degree (DD)** — average RAFT Teed and Deng [2020] optical-flow magnitude; rewards non-static videos. Reported in  $[0, 100]$  following the official VBench convention.
- **Aesthetic Quality (AQ)** — per-frame LAION aesthetic predictor score, averaged temporally.
- **Imaging Quality (IQ)** — per-frame MUSIQ Ke et al. [2021] SPAQ-trained image-quality predictor, averaged temporally.
- **Color (Clr.)** — GRiT Wu et al. [2024] caption-based color attribute alignment between the rendered subject and the color word in the prompt.

## D Additional Ablation Study on CFG Removal

Table 3: Ablation on the removal of classifier-free guidance (CFG).

Variant	Inference	FVD↓	HD-LPIPS↑	CLIP↑
w/ 4K fine-tuning	w/ CFG	273.64	0.6612	0.3012
w/ 4K fine-tuning	w/o CFG	284.71	0.6695	0.3019
w/o 4K fine-tuning	w/ CFG	408.53	0.6398	0.3017
w/o 4K fine-tuning	w/o CFG	409.15	0.6401	0.3011

**Ablation on removing classifier-free guidance (CFG).** Since the global proxy already provides a deterministic semantic target for high-resolution denoising, we remove classifier-free guidance to improve inference efficiency. We evaluate this design both with and without optional 4K fine-tuning. As shown in Table 3, disabling CFG has no significant impact on the quantitative metrics in either setting. Meanwhile, it nearly halves the DiT inference cost by eliminating the unconditional generation branch. We therefore disable CFG in our final generation pipeline.

## E Broader Impact

**Positive societal impacts.** **AtlasVid** lowers the barrier to ultra-high-resolution long-video generation by training on as few as two consumer-class GPUs (RTX Pro 6000) at 720P resolution and transferring directly to 4K and beyond. This has several positive implications. (i) It democratizes high-resolution video synthesis, making it practical for academic groups, independent creators, and non-profit educational projects that cannot afford clusters of 32–64 H-class GPUs. (ii) It reduces the energy and carbon footprint of training and serving UHR video models by an order of magnitude, since the dominant cost — quadratic spatiotemporal attention — is replaced with a locality-preserving variant whose attention FLOPs grow linearly in the number of spatiotemporal cubes. (iii) It can support accessibility applications such as automatic generation of high-quality educational visuals, sign-language interpretation videos, or visualisations for the visually-impaired community where high spatial detail matters.

**Potential negative societal impacts.** Like all powerful generative video systems, **AtlasVid** could in principle be misused for (i) producing photorealistic disinformation or non-consensual synthetic media (“deepfakes”), (ii) generating misleading long-form footage of public figures or events, or (iii) bypassing moderation tools that were trained on lower-resolution synthetic content. Because our framework is specifically designed to scale long-horizon and ultra-high-resolution synthesis, the resulting outputs are harder to distinguish from real footage than those of short low-resolution generators, which sharpens the dual-use concern.